Environmental Pollution 268 (2021) 115784

Contents lists available at ScienceDirect

Environmental Pollution

journal homepage: www.elsevier.com/locate/envpol

Critical window of exposure of CMIT/MIT with respect to developmental effects on zebrafish embryos: Multi-level endpoint and proteomics analysis☆

Nivedita Chatterjee [a], Hyunho Lee [a], Jiwan Kim [a], Doeun Kim [b], Sangkyu Lee [b], Jinhee Choi [a, *]

[a] School of Environmental Engineering, University of Seoul, 163 Seoulsiripdae-ro, Dongdaemun-gu, Seoul, 02504, Republic of Korea
[b] BK21 Plus KNU Multi-Omics Based Creative Drug Research Team, College of Pharmacy and Research Institute of Pharmaceutical Sciences, Kyungpook National University, Daegu, 41566, Republic of Korea

ARTICLE INFO

Article history:
Received 14 March 2020
Received in revised form
29 July 2020
Accepted 3 October 2020
Available online 6 October 2020

Keywords:
CMIT/MIT
Critical window of exposure
DNA methylation
Locomotion behavior
Proteomics
Developmental cardiac functional defects

ABSTRACT

Systemic toxicity, particularly, developmental defects of humidifier disinfectant chemicals that have caused lung injuries in Korean children, remains to be elucidated. This study evaluated the mechanisms of the adverse effects of 5-chloro-2-methyl-4-isothiazoline-3-one/2methyl-4-isothiazolin-3-one (CMIT/MIT), one of the main biocides of the Korean tragedy, and identify the most susceptible developmental stage when exposed in early life. To this end, the study was designed to analyze several endpoints (morphology, heart rate, behavior, global DNA methylation, gene expressions of DNA methyl-transferases (dnmts) and protein profiling) in exposed zebrafish (*Danio rerio*) embryos at various developmental stages. The results showed that CMIT/MIT exposure causes bent tail, pericardial edema, altered heart rates, global DNA hypermethylation and significant alterations in the locomotion behavior. Consistent with the morphological and physiological endpoints, proteomics profiling with bioinformatics analysis suggested that the suppression of cardiac muscle contractions and energy metabolism (oxidative phosphorylation) were possible pivotal underlying mechanisms of the CMIT/MIT mediated adverse effects. Briefly, multi-level endpoint analysis indicated the most susceptible window of exposure to be $\leq$ 6 hpf followed by $\leq$ 48 hpf for CMIT/MIT. These results could potentially be translated to a risk assessment of the developmental exposure effects to the humidifier disinfectants.

1. Introduction

Biocidal disinfectants are used widely in hospitals and household products (such as humidifier disinfectants) as well as in various industries (such as the food industry) (Christen et al., 2017). In November 2011, the Korea Centers for Disease Control and Prevention (KCDC) declared household humidifier disinfectants to the cause of epidemics of fatal lung injuries between 2006 and 2011 in several infants, children, and pregnant women (Huh et al., 2016; Kim et al., 2014; Koo et al., 2016; Lamichhane et al., 2019; Lee et al., 2012; Paek et al., 2015; Park et al., 2015). The principal components of these humidifier disinfectants products containing polyhexamethylene guanidine phosphate (PHMG), the most frequently used one followed by oligo (2-(2-ethoxy)ethoxyethyl) guanidinium (PGH), mixture of 5-chloro-2-methylisothiazol-3-one (CMIT)/2-methylisothiazol-3-one (MIT) and didecyldimethylammoniumchloride (DDAC) (Kim et al., 2016a,b; Kim and Choi, 2019; Lee et al., 2012; Park et al., 2017).

Since then, pulmonary diseases have been a focus in toxicological and epidemiological studies based on the chemicals used in the humidifier disinfectants (Kim et al., 2016a,b; Lee et al., 2018; Park et al., 2014; Song et al., 2018). The proposed mechanisms of PHMG were oxidative stress (Lee et al., 2019), DNA damage, cell cycle arrest, apoptosis (Park et al., 2019a,b) modulations of the NF-kB signaling pathway (Kim et al., 2015), endoplasmic reticulum stress (Kim et al., 2019), cytokines release, apoptosis (Park et al., 2018), induction of fibrosis and the epithelial-mesenchymal transition (EMT) (Park et al., 2019a,b), alterations in miRNA (Shin et al., 2018), and transcriptional profiling (Kim et al., 2017). One related

☆ This paper has been recommended for acceptance by Dr. Sarah Harmon.
* Corresponding author.
E-mail address: jinhchoi@uos.ac.kr (J. Choi).

https://doi.org/10.1016/j.envpol.2020.115784
0269-7491/

List of abbreviations

CMIT/MIT	5-chloro-2-methyl-4-isothiazoline-3-one/ 2methyl-4-isothiazolin-3-one
dpf	days-post-fertilization
EW1	exposure from 4 ± 2 hpf to 24 hpf and endpoint analysis at 96 hpf
EW2	exposure from 24 ± 2 hpf to 48 hpf and endpoint analysis at 96 hpf
EW3	exposure at 48 ± 2 hpf to 72 hpf and endpoint analysis at 96 hpf
EW4	exposure at 72 ± 2 hpf to 96 hpf and endpoint analysis at 96 hpf
EWC	exposure at 4 ± 2 hpf with continuous exposures until 96 hpf and endpoint analysis at 96 hpf
hpf	hour-post-fertilization
PHMG	polyhexamethylene guanidine phosphate
PHG	oligo (2-(2-ethoxy) ethoxyethyl guanidinium

study in adult female zebrafish gills found that exposure to PHMG for 28 days caused histopathological changes in the gills, an increase in the mRNA levels of inflammatory factors, and an increase in the mRNA levels of fibrosis factors (Oh et al., 2018).

The known toxicity mechanisms of isothiazolone biocides, which include CMIT/MIT, is the inhibition of dehydrogenase enzymes of the metabolic pathways, and in turn, perturbation of the physiological functions, such as oxygen consumption, adenosine triphosphate (ATP) synthesis, disruption of the protein thiols and free radical generation, leading to cell death. In particular, CMIT/MIT was reported to induce the formation of reactive oxygen species (ROS), GSH depletion, apoptosis, and necrosis through endoplasmic reticulum stress, mitochondrial dysfunction, and perturbation of the calcium homeostasis in human cultured cell lines (Di Stefano et al., 2006; Ettorre et al., 2003; Frosali et al., 2009). In addition to the effects on human cell lines, the induction of apoptosis was observed in the testis of the marine teleost mummichog *Fundulus heteroclitus* exposed to isothiazolone (Sea-Nine 211) (Ito et al., 2013).

Nevertheless, there is limited information on the systemic toxicity of humidifier disinfectants, including developmental toxicity, other than pulmonary diseases (Kim and Ji, 2019; Kim and Choi, 2019), even though the clinical and epidemiological studies showed that children were the most affected population (Kim et al., 2013; Yoon et al., 2015, 2017). In particular, significant airway dysfunction was evident in children with high levels of inhalation exposure to the mixture of CMIT/MIT (Cho et al., 2017). Another related study reported lung injuries associated with exposure to CMIT/MIT-containing humidifier disinfectants in five-year-old twin sisters (Lee et al., 2018). The early life stage of exposure to environmental chemicals could increase the susceptibility to an adverse outcome or disease burden in later life or disrupt the normal developmental pattern, because the early lifetime period (embryo or fetus) is more sensitive to chemicals (Boekelheide et al., 2012; Schug et al., 2011). From this perspective, it is essential to evaluate the adverse developmental effects related to humidifier disinfectant chemicals.

The zebrafish is a well-established model for examining developmental, neurotoxicity, and behavior, as well as altered epigenetic (global DNA methylation) analysis of the induced toxicity of various chemicals. The zebrafish possess all the qualities to become an alternative toxicological model, such as rapid growth, high egg yield, a short generation time, well-documented genetics, and developmental biology. In particular, the key characteristics that make zebrafish an excellent system for developmental toxicity testing are as follows: i) external development of transparent embryos facilitates the morphological assessment during development and ii) significant physiological and genetic homology with humans (Carney et al., 2006; Cavalieri and Spinelli, 2017; Dach et al., 2019; Ducharme et al., 2013; Kamstra et al., 2014; Mudbhary and Sadler, 2011).

This study used a phenotypically (morphology, physiology, and behavior) anchored proteomics approach to elucidate the underlying mechanism of toxicity after developmental exposure of embryonic zebrafish to four biocides, that included chlorpyrifos (Cp), PHMG, PGH, and CMIT/MIT. Initially, the embryos were exposed continuously from ≤6 to 96-h post-fertilization (hpf), and the LC_{20} and LC_{50} (the concentration at which 20% and 50% of exposed embryos show mortality, respectively) doses of each chemical were determined. Subsequently, CMIT/MIT was chosen for further analysis because it was one of the main humidifier disinfectants in the Korean mishap and was found to be most toxic among the four selected biocides tested. Morphological, physiological (heart rate), and global epigenetic (DNA methylation level and DNA methyltransferase gene expression) and proteomics analyses were performed at 96 hpf. Behavioral analysis was conducted at 10 dpf after exposure to CMIT/MIT at various time points, ≤6 to 24 hpf, 24 to 48 hpf, 48 to 72 hpf and 72 to 96 hpf. Finally, the multi-level results were combined to identify the most sensitive window of exposure of CMIT/MIT with respect to the adverse outcomes during early life exposure.

2. Materials and methods

2.1. Zebrafish embryo maintenance and screening with biocides

Wild-type zebrafish embryos were purchased from a commercial aquarium store (Gangnam Aquarium, Suwon, Korea), where adult fish were maintained in cultivation tanks with a water filtration system at 26 ± 1 °C. At less than the 2 hpf of obtaining the embryos, they were distributed in a 24-well plate (20 embryos per well) with/without chemicals at various concentrations of the four selected biocides: chlorpyrifos (Cp) (Sigma Aldrich, St. Louis, MO, USA), 5-chloro-2-methyl-4-isothiazoline-3-one and 2-methyl-4-isothiazolin-3-one (CMIT/MIT, 1.46%) (Sigma Aldrich, St. Louis, MO, USA), polyhexamethylene guanidine (PHMG) and oligo (2-(2-ethoxy)-ethoxyethyl)-guanidinium-chloride (PGH) (BOC Sciences, Shirley, NY, USA). The control, as well as the exposed embryos, were maintained at 26 °C ± 1 °C and 14/10 h light/dark cycle. The embryo mortality was selected as the endpoint and the lethal concentrations were calculated (LC_{10}, LC_{20}, LC_{50}, and LC_{90}) using the *drc* package in R.

2.2. CMIT/MIT exposures to various developmental windows and sample collection

Prior to exposure, the concentration of primary and secondary diluted solutions, whose dilution fractions were 0.01 and 0.00015, were analyzed by HPLC (high-performance liquid chromatography) (Table S1 and S2). The embryos (20 embryos per well in 24-well plate) were exposed to CMIT/MIT at various developmental windows and samples were collected at 96 hpf (Fig. 1). For behavioral analysis, the samples 10 days post fertilization (dpf) larvae were used. The developmental windows used in the exposures were as follows -

EW1 = exposure from 4 ± 2 hpf to 24 hpf and endpoint analysis at 96 hpf

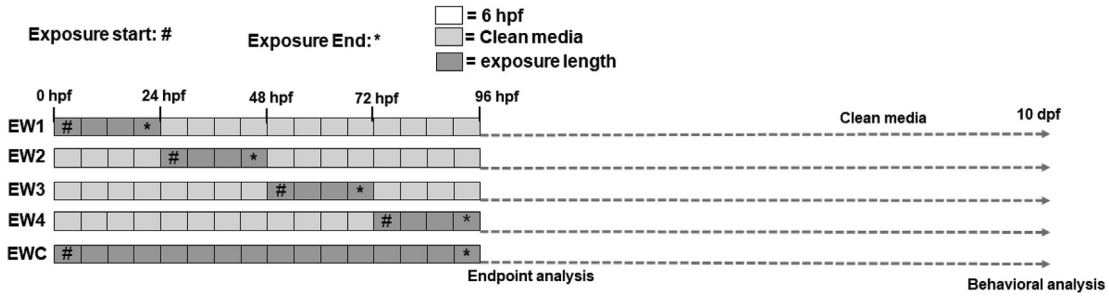

Fig. 1. Schematic diagram of various windows of exposures of CMIT/MIT and sample collection.

EW2 = exposure from 24 ± 2 hpf to 48 hpf and endpoint analysis at 96 hpf
EW3 = exposure at 48 ± 2 hpf to 72 hpf and endpoint analysis at 96 hpf
EW4 = exposure at 72 ± 2 hpf to 96 hpf and endpoint analysis at 96 hpf
EWC = exposure at 4 ± 2 hpf with continuous exposures until 96 hpf and endpoint analysis at 96 hpf

Two doses were selected for the multi-endpoints (morphology, behaviors, heart rate, DNA methylation, and related gene expressions) analysis: i) 0.25 mg/L which is ~ LC_{20} of EWC, and ii) 0.5 mg/L, which is ~LC_{50} of EWC. Only a single-dose, 0.5 mg/L, was selected for proteomics analysis.

2.3. Morphology and heart rate

Morphological defects were monitored at 96 hpf larvae under the microscope (25× magnification). The shape and size of the whole body, tail, eye and cardiac edema were mainly considered. The heartbeat was quantified from a 20-sec video collected from an individual 96 hpf larvae (three measurements for each organism, n = 20).

2.4. Global DNA methylation level

The total DNA (10 embryos per sample) was extracted using a DNA extraction kit (NucleoSpin, Macherey-Nagel GmbH & Co. KG, Germany) and the quantity and quality of DNA were detected in a NanoDrop. The global DNA methylation assays were the carried out according to the manufacturer's instructions (MethylFlash global DNA methylation, 5-mC ELISA Easy Kit, Colorimetric, epigentek; P-1030-96) and as was reported previously (Chatterjee et al., 2019).

2.5. Total RNA extraction and quantitative real-time PCR (qRT-PCR)

The total RNA was extracted from the control and treated samples (10 embryos per sample), and quality/quantity checking and cDNA synthesis were conducted as described previously (Im et al., 2019). The IQ™ SYBR Green SuperMix (Bio-Rad) reagent was used for the RT-PCR reaction and the analysis was calculated using the CFX Manager (Bio-Rad). The primers, constructed in Primer3 plus, used in the present study, are provided in supplementary materials (Table S3). The gene β-actin was used as a housekeeping gene.

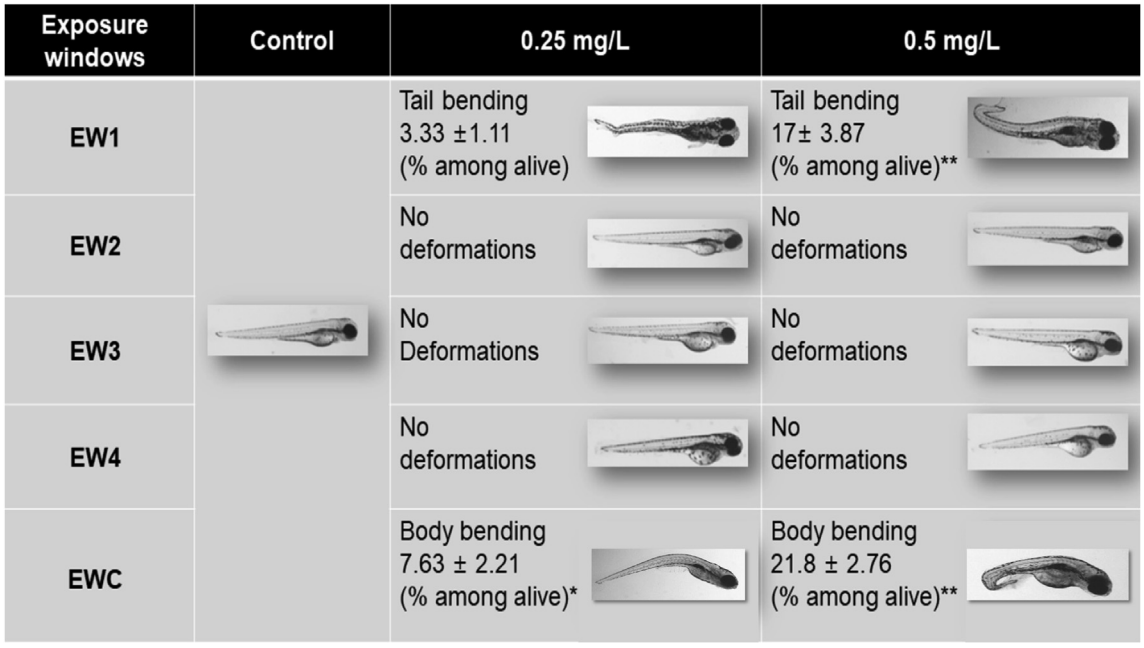

Fig. 2. Morphological changes, particularly bent tail and body bending, at various windows of exposed zebrafish embryos at two different concentrations (0.25 mg/L and 0.5 mg/L). The results are reported as the data ±SEM, *$p < 0.05$, **$p < 0.001$, n = 10.

Exposure windows	Control (beats / min.)	0.25 mg/L (beats / min.)	0.5 mg/L (beats / min.)
EW1	201.1 ± 2.2	169.4 ± 3.2***	129.4 ± 2.4***
EW2		192.2 ± 3.4*	182.2 ± 4.2**
EW3		181.2 ± 1.5*	172.8 ± 2.2**
EW4		200.2 ± 2.8	196.7 ± 3.5
EWC		143.1 ± 1.4***	121.4 ± 2.8***

Fig. 3. Comparisons of the heart rate (beats/min) with heart morphology (at 0.5 mg/L), particularly edema in the heart (shown with arrow head), at various windows of CMIT/MIT exposed zebrafish embryos. The results are reported as the data ±SEM, *$p < 0.05$, **$p < 0.001$, ***$p < 0.0001$, n = 20.

2.6. Behavior analysis

Locomotion behavior analysis was conducted according to previously described methods (Chatterjee et al., 2019; Lee et al., 2015). The analysis conducted on day 10 larvae (10 dpf) from all exposure windows treated with CMIT/MIT at two doses, 0.25 mg/L and 0.5 mg/L. Animals-aged 10 dpf were transferred to each well of a 24-well plate and acclimated to this condition for 30 min. The camera (iphone3gs) was placed on a white panel, and two thin acrylic panels, 10 cm in height, were erected on both sides of the camera. Finally, a 24-well plate with acclimated animals was placed on top and covered with a white panel to block noise during a recording. Movement behaviors were recorded for 5 min and analyzed in the following order. 24 frame per second (fps) of originally recorded video files was converted to 4 fps through the Virtual Dub software (1.10.4, http://www.virtualdub.org/), namely a total of 1200 frames and a time interval of 0.25 s between frames. The converted file was input into the Image J program (https://imagej.net/Welcome) for thresholding, binarization, and, ultimately, the extraction of coordinates of an objective (fish). Based on extracted x, y coordinates, movement parameters were analyzed, including speed (mm/s), acceleration (mm/s^2), locomotory rate (mm/s), stop duration (s), stop number (n), turning rate (rad/s), and meander (rad/mm) using MATLAB software.

2.7. Quantitative MS-based proteomics and bioinformatics analysis

Proteomics analysis was carried out, as described previously (Chatterjee et al., 2019), after extracting the proteins from 96 hpf zebrafish embryos (96 hpf at 10 embryos per sample) exposed to CMIT/MIT at 0.5 mg/L at various developmental windows (Fig. 1). The detailed method could be found in the supplementary materials.

Bioinformatics analyses were performed in String 11.0 (for protein-protein interactions) (https://string-db.org/) and DAVID (used for gene ontology analysis, biological pathways and protein classification) (https://david.ncifcrf.gov/home.jsp) with the selected proteins (fold changes > 1.5 or < 0.66) of differentially regulated proteins between control vs. exposed).

2.8. Statistical analysis

The significance of differences among/between the treatments was determined by a one-way analysis of the variance (ANOVA) followed by a post-hoc test (Tukey, $p < 0.05$) in SPSS 12.0KO (SPSS Inc., Chicago, Il, USA). A comparative Venn diagram of proteomics results was made from the open-access source 'jvenn' (Bardou et al., 2014).

3. Results and discussion

This study aimed to identify the sensitive developmental period and evaluate its underlying mechanisms while exposed to CMIT/MIT based on morphological, physiological, behavioral, epigenetic, and proteomic profile alterations in zebrafish model systems. CMIT/MIT was chosen after screening the four biocides: Cp, CMIT/MIT, PGH, and PHMG. The rationale of the selection of the three chemicals (CMIT/MIT, PGH, and PHMG) was that all three were components of disinfectants, which were responsible for the Korean mishap. Therefore, these three biocides and chlorpyrifos, a known biocide, were used for screening.

3.1. Morphological, physiological and toxicological effects

Among the four biocides selected, Cp, CMIT/MIT, PGH, and PHMG, CMIT/MIT was the most sensitive biocide for zebrafish embryos (Table S4 and Figure S1). Therefore, CMIT/MIT was chosen for various widows of exposures to shed light on developmental effects with a multi-level endpoint study. With respect to screening (mortality as endpoint) with various doses (0.25, 0.5, 0.75 and 1 mg/L) of CMIT/MIT at five exposure time points, the order of sensitivity of developmental windows was EWC > EW1 > EW3 > EW2 >EW4 (Table S5).

A severe bent axis was observed at 0.5 mg/L dose of CMIT/MIT of EWC, which was also dose-dependent (Fig. 2). Interestingly, early exposure, EW1, was evident by the marked bent tail in both doses

Table 1
Behavioral parameter (from line tracking movement) analysis of 10-day-exposed zebrafish larva. The exposures were conducted at various developmental windows (EW1, EW2, EW3, EW4, and EWC) with two concentrations (0.25 mg/L and 0.5 mg/L). The results are reported as the data ±SEM compared to the control (control = 1), *p < 0.05, **p < 0.001, ***p < 0.0001, n = 10.

Exposure windows	Locomotion behavior						Stop behavior				Angle behavior			
	Speed (mm/sec)		Acceleration (mm/sec^2)		Locomotion (m/sec)		Stop Duration (sec)		Stop No. (n)		Turning rate (rad/s)		Meander (rad/mm)	
	0.25 mg/L	0.5 mg/L	0.25 mg/L	0.5 mg/L	0.25 mg/L	0.5 mg/L	0.25 mg/L	0.5 mg/L	0.25 mg/L	0.5 mg/L	0.25 mg/L	0.5 mg/L	0.25 mg/L	0.5 mg/L
EW1	0.42 ± 0.08 ***	0.28 ± 0.03 ***	0.42 ± 0.08 ***	0.31 ± 0.03 ***	0.45 ± 0.07 ***	0.36 ± 0.03 ***	2.43 ± 0.46 **	2.49 ± 0.24**	1.37 ± 0.18 ***	1.83 ± 0.10 ***	1.29 ± 0.14	1.37 ± 0.07 **	3.27 ± 0.81 **	2.46 ± 0.33 **
EW2	0.89 ± 0.09	0.75 ± 0.09	0.93 ± 0.10	0.76 ± 0.09	0.88 ± 0.08	0.76 ± 0.09	1.06 ± 0.25	1.19 ± 0.23	0.92 ± 0.13	1.03 ± 0.14	1.11 ± 0.08	1.09 ± 0.06	1.35 ± 0.48	1.39 ± 0.40
EW3	0.74 ± 0.10	0.67 ± 0.10 *	0.73 ± 0.10	0.67 ± 0.10 *	0.71 ± 0.08 *	0.68 ± 0.10 *	1.05 ± 0.33	1.25 ± 0.25	0.80 ± 0.16	1.10 ± 0.15	1.08 ± 0.09	1.11 ± 0.08	1.62 ± 0.59	1.72 ± 0.48
EW4	0.92 ± 0.10	0.68 ± 0.10*	0.90 ± 0.10	0.68 ± 0.10*	0.90 ± 0.09	0.69 ± 0.09*	1.33 ± 0.36	1.69 ± 0.31	0.87 ± 0.14	1.27 ± 0.16	1.09 ± 0.07	1.20 ± 0.09	1.79 ± 0.57	2.42 ± 0.61*
EWC	0.57 ± 0.17 *	0.34 ± 0.09 **	0.54 ± 0.16 *	0.35 ± 0.08 ***	0.58 ± 0.15 *	0.41 ± 0.09 **	1.49 ± 0.27*	2.22 ± 0.16***	1.25 ± 0.16 ***	1.73 ± 0.09 ***	0.99 ± 0.07 ***	1.37 ± 0.06 ***	1.17 ± 0.16 ***	2.03 ± 0.21 ***

(0.25 and 0.5 mg/L), whereas the later windows of exposure (EW2, EW3, and EW4) were neither observed for bent axis nor bent tail (Fig. 2).

Significant dose-dependent decreases in heart rate, and heart edema were observed in all exposure windows, except EW4 (Fig. 3). Heart edema was unclear in the EW2 time point. Possible structural, as well as functional cardiac developmental issues were evident due to CMIT/MIT exposures. Similarly, the toxicity (mortality) endpoint, the order of sensitivities of exposure windows for the morphological as well as cardiac issues was EWC > EW1 > EW3 > EW2 > EW4 (Fig. 3).

In agreement with this study, the continuous exposure to PHMG from 2 hpf embryo to 7 dpf larvae caused developmental retardation, a decrease in heart rate, oxidative stress, and disruption of the thyroid hormone systems in zebrafish, with an LD_{50} of 2.12 mg/L (Kim and Ji, 2019). Decreased body length, hatching failure, slow heart rate, and morphological abnormalities (spinal deformities and pericardial edema) were reported in larval zebrafish exposed to chlorpyrifos in the early life stage (Jin et al., 2015). Triadimefon, a fungicide, was reported to have negative impacts on the cardiovascular system, as well as adverse effects on the morphological and functional aspects of zebrafish embryo (Liu et al., 2017).

3.2. CMIT/MIT exposures affect behavioral activity

Behavioral analysis was suggested to be a sensitive endpoint for the developmental toxicity screening of various environmental chemicals (Dach et al., 2019). The behavioral activities (with line tracking) were measured at on 10 dpf larvae and were analyzed as the locomotion behavior (speed, acceleration, and locomotion), stop behavior (stop duration and stop number), and angle behavior (turning rate and meander). In general, all developmental exposure windows (EW1, EW2, EW3, EW4, and EWC) showed decreased locomotion behavior, increased stop behavior, and higher angle behavior with a clear dose-dependency. The order of sensitivity, specifically for the locomotion behavior, were EW1 > EWC > EW4 > EW3 > EW2 (Table 1 and Figure S2). Similarly, chlorpyrifos (Jin et al., 2015), and carbendazim, a benzimidazole fungicide (Andrade et al., 2016), affected the locomotor or swimming behaviors of the larvae exposed at the early life stage. Tributyltin, the active ingredient of many biocides, reduces the locomotor activity in zebrafish embryos/larvae in a similar exposure pattern (from 6/8 hpf to 96 hpf) (Liang et al., 2017).

3.3. Alterations in the global DNA methylation levels and its related genes

Several environmental chemicals modify the developmental epigenome, and zebrafish embryos exposed to various chemicals have been used as a platform for screening for DNA methylation modifications (Bouwmeester et al., 2016). In general, the global DNA hypermethylation trend was evident due to exposure to CMIT/MIT, except for exposure to 0.5 mg/L at the EW3 time point (Table 2). The order of the global DNA hypermethylation trend was EWC > EW1 > EW4 > EW3 > EW2 at 0.25 mg/L dose while the order was EWC > EW1 > EW4 > EW2 > EW3 at 0.5 mg/L. On the other hand, there was no marked dose-dependency except at EWC and EW1 (Table 2). The gene expression result of related DNA methyltransferases (*dnmt1*, *dnmt3a1*, *dnmt3a2*, *dnmt3b1*, *dnmt3b2*, *dnmt3b3*, and *dnmt3b4*) showed that the activation of *dnmt1*, *dnmt3a2*, *dnmt3b1*, and *dnmt3b4* genes possibly contributed to the global DNA hypermethylation trend due to CMIT/MIT exposures (Table 2). Therefore, the maintenance of methylation (*dnmt1*) and *de novo* methylation (*dnmt3a2*, *dnmt3b1*, and *dnmt3b4*) were both

Table 2
Alterations in global DNA methylation (5 mC) levels and its related genes expressions levels, in respect of control, in CMIT/MIT exposed zebrafish embryo. The exposures were conducted at various developmental windows (EW1, EW2, EW3, EW4, and EWC) with two concentrations (0.25 mg/L and 0.5 mg/L). The results are reported as the data ±SEM compared to the control (control = 1). *$p < 0.05$.

Exposure windows		EW1		EW2		EW3		EW4		EWC	
Doses (mg/L)		0.25	0.5	0.25	0.5	0.25	0.5	0.25	0.5	0.25	0.5
Global DNA methylation (5 mC) Level (control = 1)		1.481 ± 0.706*	1.527 ± 0.957*	1.12 ± 0.398	1.24 ± 0.559	1.273 ± 0.934	1.046 ± 0.453	1.371 ± 0.762	1.421 ± 0.841*	1.432 ± 0.685*	1.682 ± 0.982*
Gene expressions (normalized in respect of control)	*dnmt1*	2.215 ± 0.592*	1.664 ± 0.802*	1.383 ± 0.748	1.339 ± 0.238	2.18 ± 0.982*	1.181 ± 0.412	1.774 ± 0.868*	1.789 ± 0.601*	2.385 ± 0.359**	1.901 ± 0.872*
	dnmt3a1	2.619 ± 0.826*	0.427 ± 0.068*	0.946 ± 0.102	0.841 ± 0.143	1.475 ± 0.561	1.368 ± 0.397	0.757 ± 0.0438	0.965 ± 0.184	0.846 ± 0.169	0.491 ± 0.074*
	dnmt3a2	2.052 ± 0.822*	2.308 ± 0.327**	1.641 ± 0.556*	1.583 ± 0.28*	2.923 ± 0.365**	1.956 ± 0.77*	1.73 ± 0.258*	1.565 ± 0.379*	2.704 ± 0.142**	2.298 ± 0.438 *
	dnmt3b1	2.071 ± 0.372*	1.892 ± 0.294*	1.727 ± 0.157*	1.275 ± 0.081	2.579 ± 0.43**	1.732 ± 0.344*	1.99 ± 0.135*	1.307 ± 0.196	3.768 ± 0.686**	1.922 ± 0.197*
	dnmt3b2	1.721 ± 0.12*	0.846 ± 0.031	0.673 ± 0.023	0.722 ± 0.046	0.798 ± 0.096	0.364 ± 0.092*	0.868 ± 0.051	0.595 ± 0.027	0.612 ± 0.075	0.556 ± 0.032*
	dnmt3b3	1.949 ± 0.138*	1.853 ± 0.28*	0.811 ± 0.027	1.735 ± 0.184*	1.779 ± 0.041*	1.921 ± 0.082*	1.308 ± 0.134	1.761 ± 0.108*	1.519 ± 0.097*	1.924 ± 0.781*
	dnmt3b4	2.939 ± 0.138**	2.429 ± 0.176**	1.631 ± 0.143*	2.076 ± 0.035*	1.802 ± 0.057*	1.676 ± 0.023*	2.091 ± 0.437*	1.932 ± 0.267*	2.671 ± 0.364**	0.375 ± 0.017**

activated under CMIT/MIT exposure conditions, specifically at the EWC and EW1 developmental window (Kamstra et al., 2014). Despite this, systematic dose dependency was not evidenced in any gene activation or suppression. As expected and similar to other endpoints, the most susceptible windows of exposure, in general, were found as to be EWC and EW1, followed by EW3 (Table 2).

3.4. Impacts on proteomics profile

The order of down-regulated differentially expressed proteins (DEPs) in various windows of exposure were EWC > EW3 > EW1 > EW2 > EW4, whereas the order of up-regulated DEPs was EWC > EW1 = EW4 > EW3 > EW2 (Fig. 4). The number of down-regulated DEPs was higher than up-regulated in each window of exposure. Among the up-regulated proteins, only six were common, whereas 17 proteins were common among the down-regulated ones at all exposure time points (Table 3 and Fig. 4). Differentially regulated (fold change > 1.5 or fold change < 0.66) proteins for each window of exposure are presented in supplementary materials. At the EW1 exposure time point, the most up-regulated and down-regulated protein were *vtg6* (1.861 fold) and *ngs* (0.309 fold), respectively (Table S6). The highest up-regulated protein and most down-regulated proteins for the EW2 exposure window were *hnrnpul1* (2.01 fold) and *ckmt2a* (0.254 fold), respectively (Table S7). In the case of EW3, the most down-regulated and up-regulated proteins were zgc:86599 (0.215 fold) and *smx5* (1.942 fold), respectively (Table S8). The highest up-regulated and down-regulated proteins in EW4 were *vtg4* (3.22 fold) and LOC101882408 (vimentin-related 1) (0.35 fold), respectively (Table S9). In the EWC exposure scenario, the highest up-regulated and most down-regulated proteins were *vtg4* (5.49 fold) and *ckmt2a* (0.137 fold), respectively (Table S10).

The most common KEGG pathways, which were down-regulated in all exposure windows, were cardiac muscle contractions, oxidative phosphorylation, gap junction, focal adhesion, phagosome, and metabolic pathways. In contrast, there were no common up-regulated KEGG pathways and cysteine and methionine metabolism came up in the EW1, EW4, and EWC exposure time points (Table 4). Figure S3 shows the 'protein-protein' interactions, specifically with their actions, of these pathways for each window of exposure (Figure S3A for EW1; Figure S3B for EW2; Figure S3C for EW3; Figure S3D for EW4; Figure S3E for EWC). A similar pattern in OMICS was observed. Transcriptome sequencing-based studies reported ECM-receptor interactions, focal adhesion, cell cycle, DNA replication, phototransduction, and adherens junction pathways to be associated with the toxicity of two pesticides, chlorpyrifos, and beta-cypermethrin, in the early life stages of zebrafish (Zhang et al., 2017). The most common down-regulated reactome pathway was respiratory electron transport (Table S11). Based on down-regulated DEPs (DAVID 6.8), the common biological processes (GO_BP) were found as to be heart contraction, microtubule-based processes, mitochondrial electron transport, and ubiquinol to cytochrome *c*. The common molecular functions (GO_MF) were cytochrome-c oxidase activity, GTPase activity, GTP binding, structural constituent of the cytoskeleton, and ubiquinol-cytochrome-c reductase activity in all exposure windows (Table S12). While based on up-regulated DEPs (DAVID 6.8), the lipid transport as a common GO_BP and lipid transporter activity as a common GO_MF were found for all exposure windows (Table S12).

Proteomics analysis showed that CMIT/MIT exposure caused the up-regulation of S-adenosyl methionine synthase (EC 2.5.1.6) (*mat1a*) and betaine–homocysteine S-methyltransferase 1 (EC

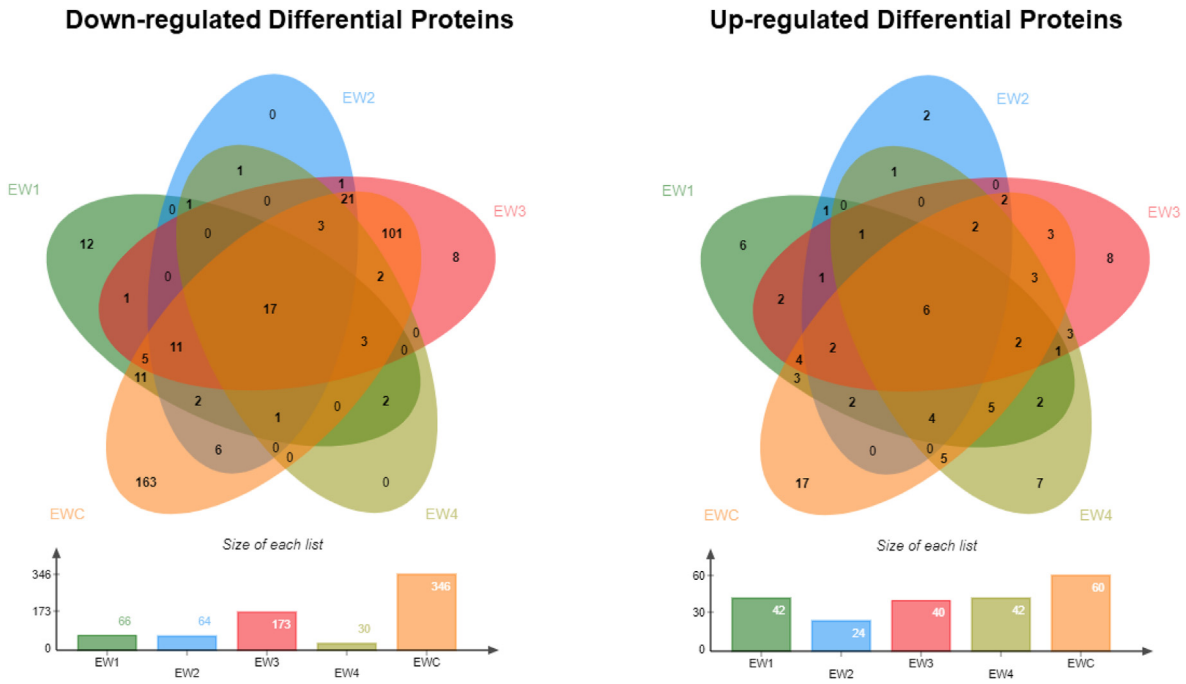

Fig. 4. Comparative analysis of differentially regulated proteins (down-regulated fold change < 0.66 and up-regulated fold change > 1.5). Proteomics analysis was conducted at various developmental windows (EW1, EW2, EW3, EW4, and EWC) in 0.5 mg/L exposed zebrafish larva (96 hpf). The Venn diagram was made in open source 'jvenn'.

2.1.1.5) (*bhmt*) proteins level (Table 3), as well as upregulation of the 'Cysteine and methionine metabolism' (Table 4), but the level varied between windows of exposure. The proteomics results supported the global DNA hypermethylation level in CMIT/MIT exposed embryos. Alterations in the S-adenosylmethionine (SAM) to S-adenosylhomocysteine (SAH) ratio and *dnmt1* expression might affect the global DNA methylation level in CMIT/MIT-exposed zebrafish embryos (Fang et al., 2013).

Among the exposure windows, EW1 (≤6 hpf to ~24 hpf) and EWC (≤6 hpf to ~96 hpf), which only differs in exposure duration, were the most sensitive time points for almost all endpoints analyzed.

In addition to mortality, EWC was found to be more sensitive than EW1 for heart functional analysis, possibly because prolonged exposure causes higher pericardial edema and high intensity of suppression of cardiac muscle contractions and calcium signaling pathway (Table 4). In contrast, the most severe alterations in behavior were observed in the EW1 developmental window. This might be because of a bent tail (morphological alterations) (Fig. 2), reduced muscle contraction (Table S12, GO_BP), decreased motor activity (Table S12, GO_MF), as well as 'ECM-receptor interaction' (Table 4), which are the only differentiated phenotype, proteins, and pathway altered in the EW1 exposure window. The ECM receptors play a key role in the neuronal structure, synaptic plasticity, and animal behavior by modulating the downstream signaling cascades that control the cytoskeletal dynamics and synaptic activity (Kerrisk et al., 2014). Suppression of the 'tight-junction' pathway was only evidenced in two developmental time points, EW1 and EWC; both are early windows of exposure. The 'Phototransduction' pathway was also down-regulated in EWC, which shows that alterations of vision might also affect the behavior of the larvae at the EWC window (Table 4). In general, suppression of cardiac muscle contraction, down-regulated energy metabolism (Table 4), and decreased heart rate (Fig. 3) affect the locomotion behavior of the larvae.

The highest toxicity in EWC was attributed mainly to the longer time of exposure (~90 h), while all other windows only received ≤ 24 h of exposure. Interestingly, EW3 (48–72 hpf) was more sensitive than EW2 and EW4. This is because the candidate proteins might not become functional until 48 hpf for the CMIT/MIT interaction and toxicity (Bardet et al., 2002; Chen et al., 2014). Proteins related to cardiac muscle tissue development and aerobic respiration (Table S12, GO_BP) were only down-regulated in EW3. Moreover, proteins involved in ion transport by ATPases, ion homeostasis, and calcium pathway were suppressed in EW3 and EWC (Table S11). Possibly these proteins played an important role in cardiac dysfunction at EW3. Nevertheless, future studies will be needed to explain the exposure window of sensitivity.

4. Conclusions

This study examined the toxicity mechanisms and susceptible developmental stage of CMIT/MIT by analyzing several endpoints (morphology, heart rate, behavior, global DNA methylation, and protein profiling) in zebrafish embryos. EW1 (≤6 hpf to ~ 24 hpf) and EWC (≤6 hpf to ~ 96 hpf) were found to be the most sensitive exposure windows. Overall, early life exposure of CMIT/MIT not only causes lung (breathing) problems in humans, it also causes cardiac functional failure as well as behavioral alterations in zebrafish, which might be translated to humans. Therefore, this study would directly support a risk assessment and human extrapolation of CMIT/MIT exposure, specifically regarding developmental toxicity.

Author statement

Chatterjee Nivedita: Writing- Original Draft, Investigation, Visualization, Data Curation. Hyunho Lee: Investigation. Jiwan Kim: Writing- Reviewing and Editing. Doeun Kim: Formal analysis. Sangkyu Lee: Formal analysis, Writing- Reviewing and Editing. Jinhee Choi: Supervision, Conceptualization, Writing- Reviewing and Editing.

Table 3
Common differentially regulated (fold change > 1.5 or fold change < 0.66) proteins. Proteomics analysis was conducted at various developmental windows (EW1, EW2, EW3, EW4, and EWC) in 0.5 mg/L exposed zebrafish larva (96 hpf).

Protein ID	Protein name	Gene Name	Fold Changes in various exposure windows (*p*-value)				
			EW1	EW2	EW3	EW4	EWC
Down-regulated Proteins							
Q15I84	Crystallin gamma EM2-5 (Crystallin, gamma M2d5)	crygm2d5	0.408 (0.918E-05)	0.349 (2.95E-05)	0.266 (1.22E-05)	0.452 (0.0001863)	0.215 (7.37E-06)
Q5U3G0	Progesterone receptor membrane component 1	pgrmc1	0.457 (0.013382)	0.618 (0.000417)	0.314 (4.37E-6)	0.616 (0.0003716)	0.197 (1.84E-06)
E7F2H3	MutS homolog 4	msh4	0.459 (0.322887)	0.409 (0.345003)	0.457 (0.360968)	0.634 (0.5250266)	0.247 (0.160606)
Q7ZUU6	Creatine kinase, mitochondrial 2a (sarcomeric) (Zgc:56085)	ckmt2a	0.489 (0.180901)	0.255 (0.075215)	0.271 (0.06567)	0.388 (0.1383686)	0.137 (0.042981)
F1R4K1	Tubulin beta chain	zgc:153426	0.497 (0.000901)	0.624 (0.006689)	0.316 (0.000206)	0.542 (0.0015405)	0.177 (6.65E-05)
Q45FX9	BetaA2-2-crystallin (Crystallin, beta A2b)	cryba2b	0.505 (0.000265)	0.488 (0.00018)	0.331 (3.08E-05)	0.568 (0.000406)	0.279 (2.06E-05)
Q6PE34	Tubulin beta chain	zgc:65894	0.514 (0.010068)	0.602 (0.019145)	0.336 (0.000756)	0.595 (0.0180605)	0.283 (0.000696)
F1QGY8	Glycoprotein M6Bb	gpm6bb	0.533 (9.18E-05)	0.559 (2.95E-05)	0.332 (1.22E-05)	0.595 (0.0001863)	0.209 (7.37E-06)
A0A0R4IPH2	Tubulin beta chain	tubb4b	0.533 (0.013382)	0.658 (0.000417)	0.303 (0.005604)	0.595 (0.0062049)	0.204 (0.002655)
Q4VBV1	Cytochrome *b-c*1 complex subunit 7	uqcrb	0.574 (0.03271)	0.497 (0.015675)	0.374 (0.004147)	0.592 (0.320619)	0.281 (0.001984)
F1R1J3	Zgc:86599 (Fragment)	zgc:86599	0.585 (0.020947)	0.559 (0.022348)	0.215 (0.001272)	0.452 (0.0093367)	0.179 (0.000798)
F1QJ56	NADH:ubiquinone oxidoreductase subunit B10	ndufb10	0.602 (0.005178)	0.551 (0.00157)	0.426 (0.000622)	0.607 (0.0078742)	0.285 (0.000339)
F1QEJ5	Ubiquinol-cytochrome c reductase, complex III subunit VII	uqcrq	0.631 (0.026578)	0.531 (0.015521)	0.421 (0.001934)	0.664 (0.0330553)	0.301 (0.000326)
Q6WFZ4	Metaxin 2 (Mtx2 protein)	mtx2	0.424 (0.000155)	0.416 (0.000596)	0.267 (0.000112)	0.476 (0.0017275)	0.186 (3.61E-06)
Q9W6A5	Green-sensitive opsin-1 (Green cone photoreceptor pigment 1) (Opsin RH2-1)	opn1mw1	0.627 (0.004759)	0.520 (0.002401)	0.395 (0.000101)	0.648 (0.0117798)	0.235 (0.000101)
Q6ZM23	Cytochrome *c* oxidase subunit VIc	cox6c	0.663 (0.024906)	0.628 (0.019949)	0.474 (0.007803)	0.662 (0.0318571)	0.415 (0.007835)
F8W5Z1	Retinoschisin 1a	rs1a	0.665 (0.0113393)	0.543 (0.016768)	0.552 (0.024977)	0.644 (0.00792989)	0.398 (0.006153)
Up-regulated Proteins							
F1QQQ3	Vitellogenin 3, phosvitinless	vtg3	1.601 (0.0070672)	1.752 (0.03786)	1.780 (0.023313)	2.383 (0.0066875)	3.262 (0.000381)
Q1L9A1	Heterogeneous nuclear ribonucleoprotein U-like 1	hnrnpul1	1.778 (0.00561163)	2.007 (0.00635245)	1.532 (0.0072517)	1.663 (0.005472563)	2.078 (0.00829883)
A0A0R4IUA0		vtg7	1.733 (0.036336)	1.846 (0.016804)	1.531 (0.0140564)	2.814 (0.005575)	4.817 (0.0045885)
F1QV15	Vitellogenin 6 (Fragment)	vtg6	1.861 (0.0082749)	1.977 (0.007832)	1.820 (0.028674)	3.169 (0.0097018)	5.335 (0.001802)
Q5RKP8	U6 snRNA-associated Sm-like protein LSm2	smx5	1.596 (0.0043336)	1.515 (0.0067591)	1.942 (0.023722)	1.869 (0.0056211)	1.639 (0.0040765)
Q1ED27	DnaJ (Hsp40) homolog, subfamily C, member 8 (Zgc:136281)	dnajc8	1.522 (0.0058063)	1.578 (0.007553)	1.585 (0.0046255)	1.558 (0.00645724)	1.983 (0.0286021)
Global methylation (DNA) related Proteins							
Q7ZW04	S-adenosyl methionine synthase (EC 2.5.1.6)	mat1a	1.543 (0.0034852)	1.382 (0.005044)	1.284 (0.030264)	1.522 (0.0041953)	1.618 (0.019413)
Q32LQ4	Betaine–homocysteine S-methyltransferase 1 (EC 2.1.1.5)	Bhmt	1.502 (0.016182)	1.347 (0.004296)	1.208 (0.016002)	1.539 (0.0207168)	1.522 (0.015709)

Table 4
KEGG pathway analysis based on STRING 11.0 with differentially regulated (fold change > 1.5 or fold change < 0.66) proteins. Proteomics analysis was conducted at various developmental windows (EW1, EW2, EW3, EW4, and EWC) in 0.5 mg/L exposed zebrafish larva (96 hpf).

KEGG Pathways		Count in gene set				
Down-regulated (fold change < 0.66) differentially altered protein						
Pathway	Description	EW1	EW2	EW3	EW4	EWC
dre04260	Cardiac muscle contraction	6 of 89	4 of 89	14 of 89	4 of 89	17 of 89
dre00190	Oxidative phosphorylation	6 of 130	7 of 130	27 of 130	5 of 130	31 of 130
dre04540	Gap junction	4 of 123	3 of 123	6 of 123	4 of 123	8 of 123
dre04510	Focal adhesion	5 of 236	4 of 236	7 of 236	4 of 236	9 of 236
dre04145	Phagosome	4 of 142	4 of 142	8 of 142	5 of 142	13 of 142
dre01100	Metabolic pathways	8 of 1278	9 of 1278	37 of 1278	6 of 1278	52 of 1278
dre03050	Proteasome	2 of 51	4 of 51	5 of 51		12 of 51
dre04810	Regulation of actin cytoskeleton		4 of 251		3 of 251	9 of 251
dre04520	Adherens junction			4 of 95	2 of 95	5 of 95
dre04530	Tight junction	3 of 203				8 of 203
dre04310	Wnt signaling pathway		3 of 170		2 of 170	
dre04370	VEGF signaling pathway		2 of 71		2 of 71	
dre03010	Ribosome			7 of 126		10 of 126
dre00410	beta-Alanine metabolism			4 of 34		3 of 34
dre04512	ECM-receptor interaction	4 of 82				
dre00330	Arginine and proline metabolism		2 of 58			
dre04020	Calcium signaling pathway					12 of 245
dre04261	Adrenergic signaling in cardiomyocytes					9 of 180
dre04216	Ferroptosis					4 of 42
dre00071	Fatty acid degradation					4 of 44
dre04217	Necroptosis					7 of 152
dre01200	Carbon metabolism					6 of 125
dre05132	Salmonella infection					5 of 91
dre04744	Phototransduction					3 of 32
dre04621	NOD-like receptor signaling pathway					6 of 140
dre00020	Citrate cycle (TCA cycle)					3 of 32
Up-regulated (fold change > 1.5) differentially altered proteins						
dre00270	Cysteine and methionine metabolism	2 of 47			3 of 47	2 of 47
dre00260	Glycine, serine and threonine metabolism	2 of 45	2 of 45			2 of 45
dre00970	Aminoacyl-tRNA biosynthesis					4 of 39
dre04216	Ferroptosis					2 of 42
dre03320	PPAR signaling pathway					2 of 68
dre03030	DNA replication					2 of 38
dre00983	Drug metabolism - other enzymes					2 of 61
dre00982	Drug metabolism - cytochrome P450					2 of 33
dre00980	Metabolism of xenobiotics by cytochrome P450					2 of 35
dre00480	Glutathione metabolism					2 of 54

Funding

This work was supported by the Mid-career Researcher Program (2017R1A2B3002242) through the National Research Foundation of Korea (NRF) funded by the Ministry of Science and ICT, South Korea.

Declaration of competing interest

The authors declare that they have no known competing financial interests or personal relationships that could have appeared to influence the work reported in this paper.

Appendix A. Supplementary data

Supplementary data to this article can be found online at https://doi.org/10.1016/j.envpol.2020.115784.

References

Andrade, T.S., Henriques, J.F., Almeida, A.R., Machado, A.L., Koba, O., Giang, P.T., Soares, A.M.V.M., Domingues, I., 2016. Carbendazim exposure induces developmental, biochemical and behavioural disturbance in zebrafish embryos. Aquat. Toxicol. 170, 390–399. https://doi.org/10.1016/j.aquatox.2015.11.017.

Bardet, P.L., Horard, B., Robinson-Rechavi, M., Laudet, V., Vanacker, J.M., 2002. Characterization of oestrogen receptors in zebrafish (Danio rerio). J. Mol. Endocrinol. 153–163. https://doi.org/10.1677/jme.0.0280153.

Bardou, P., Mariette, J., Escudié, F., Djemiel, C., Klopp, C., 2014. jvenn: an interactive Venn diagram viewer. BMC Bioinf. 15, 293. https://doi.org/10.1186/1471-2105-15-293.

Boekelheide, K., Blumberg, B., Chapin, R.E., Cote, I., Graziano, J.H., Janesick, A., Lane, R., Lillycrop, K., Myatt, L., States, J.C., Thayer, K.A., Waalkes, M.P., Rogers, J.M., 2012. Predicting later-life outcomes of early-life exposures. Environ. Health Perspect. 120, 1353–1361. https://doi.org/10.1289/ehp.1204934.

Bouwmeester, M.C., Ruiter, S., Lommelaars, T., Sippel, J., Hodemaekers, H.M., van den Brandhof, E.-J., Pennings, J.L.A., Kamstra, J.H., Jelinek, J., Issa, J.-P.J., Legler, J., van der Ven, L.T.M., 2016. Zebrafish embryos as a screen for DNA methylation modifications after compound exposure. Toxicol. Appl. Pharmacol. 291, 84–96. https://doi.org/10.1016/j.taap.2015.12.012.

Carney, S.A., Prasch, A.L., Heideman, W., Peterson, R.E., 2006. Understanding dioxin developmental toxicity using the zebrafish model. Birth Defects Res. Part A Clin. Mol. Teratol. 76, 7–18. https://doi.org/10.1002/bdra.20216.

Cavalieri, V., Spinelli, G., 2017. Environmental epigenetics in zebrafish. Epigenet. Chromatin 10, 46. https://doi.org/10.1186/s13072-017-0154-0.

Chatterjee, N., Choi, S., Kwon, O.K., Lee, S., Choi, J., 2019. Multi-generational impacts of organic contaminated stream water on Daphnia magna: a combined proteomics, epigenetics and ecotoxicity approach. Environ. Pollut. 249, 217–224. https://doi.org/10.1016/j.envpol.2019.03.028.

Chen, J., Tanguay, R.L., Tal, T.L., Gai, Z., Ma, X., Bai, C., Tilton, S.C., Jin, D., Yang, D., Huang, C., Dong, Q., 2014. Early life perfluorooctanesulphonic acid (PFOS) exposure impairs zebrafish organogenesis. Aquat. Toxicol. 150, 124–132. https://doi.org/10.1016/j.aquatox.2014.03.005.

Cho, H.-J., Park, D.-U., Yoon, J., Lee, E., Yang, S.-I., Kim, Y.-H., Lee, S.-Y., Hong, S.-J., 2017. Effects of a mixture of chloromethylisothiazolinone and methylisothiazolinone on peripheral airway dysfunction in children. PloS One 12. https://doi.org/10.1371/journal.pone.0176083 e0176083–e0176083.

Christen, V., Faltermann, S., Brun, N.R., Kunz, P.Y., Fent, K., 2017. Cytotoxicity and molecular effects of biocidal disinfectants (quaternary ammonia, glutaraldehyde, poly(hexamethylene biguanide) hydrochloride PHMB) and their mixtures in vitro and in zebrafish eleuthero-embryos. Sci. Total Environ. 586, 1204–1218. https://doi.org/10.1016/j.scitotenv.2017.02.114.

Dach, K., Yaghoobi, B., Schmuck, M.R., Carty, D.R., Morales, K.M., Lein, P.J., 2019. Teratological and behavioral screening of the national toxicology program 91-compound library in zebrafish (Danio rerio). Toxicol. Sci. 167, 77–91. https://doi.org/10.1093/toxsci/kfy266.

Di Stefano, A., Frosali, S., Leonini, A., Ettorre, A., Priora, R., Di Simplicio, F.C., Di Simplicio, P., 2006. GSH depletion, protein S-glutathionylation and mitochondrial transmembrane potential hyperpolarization are early events in initiation of cell death induced by a mixture of isothiazolinones in HL60 cells. Biochim. Biophys. Acta Mol. Cell Res. 1763, 214–225. https://doi.org/10.1016/j.bbamcr.2005.12.012.

Ducharme, N.A., Peterson, L.E., Benfenati, E., Reif, D., McCollum, C.W., Gustafsson, J.-Å., Bondesson, M., 2013. Meta-analysis of toxicity and teratogenicity of 133 chemicals from zebrafish developmental toxicity studies. Reprod. Toxicol. 41, 98–108. https://doi.org/10.1016/j.reprotox.2013.06.070.

Ettorre, A., Neri, P., Di Stefano, A., Andreassi, M., Anselmi, C., Andreassi, L., 2003. Involvement of oxidative stress in apoptosis induced by a mixture of isothiazolinones in normal human keratinocytes. J. Invest. Dermatol. 121, 328–336. https://doi.org/10.1046/j.1523-1747.2003.12360.x.

Fang, X., Corrales, J., Thornton, C., Scheffler, B.E., Willett, K.L., 2013. Global and gene specific DNA methylation changes during zebrafish development. Comp. Biochem. Physiol. B Biochem. Mol. Biol. 166, 99–108. https://doi.org/10.1016/j.cbpb.2013.07.007.

Frosali, S., Leonini, A., Ettorre, A., Di Maio, G., Nuti, S., Tavarini, S., Di Simplicio, P., Di Stefano, A., 2009. Role of intracellular calcium and S-glutathionylation in cell death induced by a mixture of isothiazolinones in HL60 cells. Biochim. Biophys. Acta Mol. Cell Res. 1793, 572–583. https://doi.org/10.1016/j.bbamcr.2008.11.018.

Huh, J.W., Hong, S.B., Do, K.H., Koo, H.J., Jang, S.J., Lee, M.S., Paek, D., Park, D.U., Lim, C.M., Koh, Y., 2016. Inhalation lung injury associated with humidifier disinfectants in adults. J. Kor. Med. Sci. 31, 1857–1862. https://doi.org/10.3346/jkms.2016.31.12.1857.

Im, J., Chatterjee, N., Choi, J., 2019. Genetic, epigenetic, and developmental toxicity of Chironomus riparius raised in metal-contaminated field sediments: a multigenerational study with arsenic as a second challenge. Sci. Total Environ. 672, 789–797. https://doi.org/10.1016/j.scitotenv.2019.04.013.

Ito, M., Mochida, K., Ito, K., Onduka, T., Fujii, K., 2013. Induction of apoptosis in testis of the marine teleost mummichog Fundulus heteroclitus after in vivo exposure to the antifouling biocide 4,5-dichloro-2-n-octyl-3(2H)-isothiazolone (Sea-Nine 211). Chemosphere 90, 1053–1060. https://doi.org/10.1016/j.chemosphere.2012.08.052.

Jin, Y., Liu, Z., Peng, T., Fu, Z., 2015. The toxicity of chlorpyrifos on the early life stage of zebrafish: a survey on the endpoints at development, locomotor behavior, oxidative stress and immunotoxicity. Fish Shellfish Immunol. 43, 405–414. https://doi.org/10.1016/j.fsi.2015.01.010.

Kamstra, J.H., Aleström, P., Kooter, J.M., Legler, J., 2014. Zebrafish as a model to study the role of DNA methylation in environmental toxicology. Environ. Sci. Pollut. Res. 22, 16262–16276. https://doi.org/10.1007/s11356-014-3466-7.

Kerrisk, M.E., Cingolani, L.A., Koleske, A.J., 2014. ECM receptors in neuronal structure, synaptic plasticity, and behavior. Prog. Brain Res. 214, 101–131. https://doi.org/10.1016/B978-0-444-63486-3.00005-0.

Kim, H.-R., Hwang, G.-W., Naganuma, A., Chung, K.-H., 2016a. Adverse health effects of humidifier disinfectants in Korea: lung toxicity of polyhexamethylene guanidine phosphate. J. Toxicol. Sci. 41, 711–717. https://doi.org/10.2131/jts.41.711.

Kim, H., Ji, K., 2019. Exposure to humidifier disinfectants induces developmental effects and disrupts thyroid endocrine systems in zebrafish larvae. Ecotoxicol. Environ. Saf. 184, 109663. https://doi.org/10.1016/j.ecoenv.2019.109663.

Kim, H.J., Lee, M.-S., Hong, S.-B., Huh, J.W., Do, K.-H., Jang, S.J., Lim, C.-M., Chae, E.J., Lee, H., Jung, M., Park, Y.-J., Park, J.-H., Kwon, G.-Y., Gwack, J., Youn, S.-K., Kwon, J.-W., Yang, B.-G., Jun, B.-Y., Kim, Y., Cheong, H.-K., Chun, B.C., Kim, H., Lee, K., Koh, Y., 2014. A cluster of lung injury cases associated with home humidifier use: an epidemiological investigation. Thorax 69, 703–708. https://doi.org/10.1136/thoraxjnl-2013-204132.

Kim, H.R., Lee, K., Park, C.W., Song, J.A., Shin, D.Y., Park, Y.J., Chung, K.H., 2016b. Polyhexamethylene guanidine phosphate aerosol particles induce pulmonary inflammatory and fibrotic responses. Arch. Toxicol. 90, 617–632. https://doi.org/10.1007/s00204-015-1486-9.

Kim, H.R., Shin, D.Y., Chung, K.H., 2015. The role of NF-κB signaling pathway in polyhexamethylene guanidine phosphate induced inflammatory response in mouse macrophage RAW264.7 cells. Toxicol. Lett. 233, 148–155. https://doi.org/10.1016/j.toxlet.2015.01.005.

Kim, K.W., Ahn, K., Yang, H.J., Lee, S.Y., Park, J.D., Kim, W.K., Kim, J.-T., Kim, H.H., Rha, Y.H., Park, Y.M., Sohn, M.H., Oh, J.-W., Lee, H.R., Lim, D.H., Choung, J.T., Han, M.Y., Lee, E., Kim, H.-Y., Seo, J.-H., Kim, B.-J., Cho, Y.A., Do, K.-H., Kim, S.-A., Jang, S.-J., Lee, M.-S., Kim, H.-J., Kwon, G.-Y., Park, J.-H., Gwack, J., Youn, S.-K., Kwon, J.-W., Jun, B.-Y., Pyun, B.Y., Hong, S.-J., 2013. Humidifier disinfectant-associated children's interstitial lung disease. Am. J. Respir. Crit. Care Med. 189 (1), 48–56. https://doi.org/10.1164/rccm.201306-1088oc.

Kim, M.-S., Jeong, S.W., Choi, S.-J., Han, J.-Y., Kim, S.-H., Yoon, S., Oh, J.-H., Lee, K., 2017. Analysis of genomic responses in a rat lung model treated with a humidifier sterilizer containing polyhexamethyleneguanidine phosphate. Toxicol. Lett. 268, 36–43. https://doi.org/10.1016/j.toxlet.2016.11.005.

Kim, S.H., Kwon, D., Lee, S., Ki, S.H., Jeong, H.G., Hong, J.T., Lee, Y.-H., Jung, Y.-S., 2019. Polyhexamethyleneguanidine phosphate-induced cytotoxicity in liver cells is alleviated by tauroursodeoxycholic acid (TUDCA) via a reduction in endoplasmic reticulum stress. Cells 8, 1023. https://doi.org/10.3390/cells8091023.

Kim, Y., Choi, J., 2019. Early life exposure of a biocide, CMIT/MIT causes metabolic toxicity via the O-GlcNAc transferase pathway in the nematode C. elegans. Toxicol. Appl. Pharmacol. 376, 1–8. https://doi.org/10.1016/j.taap.2019.05.012.

Koo, H.J., Do, K.-H., Chae, E.J., Kim, H.J., Song, J.S., Jang, S.J., Hong, S.-B., Huh, J.W., Lee, E., Hong, S.-J., 2016. Humidifier disinfectant-associated lung injury in adults: prognostic factors in predicting short-term outcome. Eur. Radiol. 27, 203–211. https://doi.org/10.1007/s00330-016-4367-6.

Lamichhane, D.K., Leem, J.-H., Lee, S.-M., Yang, H.-J., Kim, J., Lee, J.-H., Ko, J.K., Kim, H.C., Park, D.-U., Cheong, H.-K., 2019. Family-based case-control study of exposure to household humidifier disinfectants and risk of idiopathic interstitial pneumonia. PloS One 14. https://doi.org/10.1371/journal.pone.0221322 e0221322–e0221322.

Lee, E., Son, S.K., Yoon, J., Cho, H.J., Yang, S.I., Jung, S., Do, K.H., Cho, Y.A., Lee, S.Y., Park, D.U., Hong, S.J., 2018. Two cases of chloromethylisothiazolinone and methylisothiazolinone-associated toxic lung injury. J. Kor. Med. Sci. 33, e119. https://doi.org/10.3346/jkms.2018.33.e119.

Lee, J.-H., Kim, Y.-H., Kwon, J.-H., 2012. Fatal misuse of humidifier disinfectants in Korea: importance of screening risk assessment and implications for management of chemicals in consumer products. Environ. Sci. Technol. 46, 2498–2500. https://doi.org/10.1021/es300567j.

Lee, S.-B., Choe, Y., Chon, T.-S., Kang, H.Y., 2015. Analysis of zebrafish (Danio rerio) behavior in response to bacterial infection using a self-organizing map. BMC Vet. Res. 11, 269. https://doi.org/10.1186/s12917-015-0579-2.

Lee, Y.-H., Seo, D.-S., Lee, M.J., Cha, H.-G., 2019. Immunohistochemical characterization of oxidative stress in the lungs of rats exposed to the humidifier disinfectant polyhexamethylene guanidine hydrochloride. J. Toxicol. Pathol. 32, 311–317. https://doi.org/10.1293/tox.2019-0049.

Liang, X., Souders, C.L., Zhang, J., Martyniuk, C.J., 2017. Tributyltin induces premature hatching and reduces locomotor activity in zebrafish (Danio rerio) embryos/larvae at environmentally relevant levels. Chemosphere 189, 498–506. https://doi.org/10.1016/j.chemosphere.2017.09.093.

Liu, H., Chu, T., Chen, L., Gui, W., Zhu, G., 2017. The cardiovascular toxicity of triadimefon in early life stage of zebrafish and potential implications to human health. Environ. Pollut. 231, 1093–1103. https://doi.org/10.1016/j.envpol.2017.05.072.

Mudbhary, R., Sadler, K.C., 2011. Epigenetics, development, and cancer: zebrafish make their mark. Birth Defects Res. C. Embryo Today 93, 194–203. https://doi.org/10.1002/bdrc.20207.

Oh, H., Kim, C.-Y., Ryu, B., Kim, U., Kim, J., Lee, J.-M., Lee, B.-H., Moon, J., Jung, C., Park, J.-H., 2018. Respiratory toxicity of polyhexamethylene guanidine phosphate exposure in zebrafish. Zebrafish 15, 460–472. https://doi.org/10.1089/zeb.2018.1571.

Paek, D., Koh, Y., Park, D.U., Cheong, H.K., Do, K.H., Lim, C.M., Hong, S.J., Kim, Y.H., Leem, J.H., Chung, K.H., Choi, Y.Y., Lee, J.H., Lim, S.Y., Chung, E.H., Cho, Y.A., Chae, E.J., Joh, J.S., Yoon, Y., Lee, K.H., Choi, B.Y., Gwack, J., 2015. Nationwide study of humidifier disinfectant lung injury in South Korea, 1994-2011 incidence and dose-response relationships. Ann. Am. Thorac. Soc. 12, 1813–1821. https://doi.org/10.1513/AnnalsATS.201504-221OC.

Park, D.-U., Choi, Y.-Y., Ahn, J.-J., Lim, H.-K., Kim, S.-K., Roh, H.-S., Cheong, H.-K., Leem, J.-H., Koh, D.-H., Jung, H.-J., Lee, K.-M., Lee, J.-H., Kim, Y.-H., Lim, S.-Y., Paek, D.-M., Lim, C.-M., Hong, S.-J., 2015. Relationship between exposure to household humidifier disinfectants and risk of lung injury: a family-based study. PloS One 10. https://doi.org/10.1371/journal.pone.0124610.

Park, D., Leem, J., Lee, K., Lim, H., Choi, Y., Ahn, J.-J., Lim, S., Park, J., Choi, K., Lee, N., Jung, H., Ha, J., Paek, D., 2014. Exposure characteristics of familial cases of lung injury associated with the use of humidifier disinfectants. Environ. Health 13, 70. https://doi.org/10.1186/1476-069X-13-70.

Park, D.U., Ryu, S.H., Lim, H.K., Kim, S.K., Choi, Y.Y., Ahn, J.J., Lee, E., Hong, S.B., Do, K.H., Cho, J. lim, Bae, M.J., Shin, D.C., Paek, D.M., Hong, S.J., 2017. Types of household humidifier disinfectant and associated risk of lung injury (HDLI) in South Korea. Sci. Total Environ. 53–60. https://doi.org/10.1016/j.scitotenv.2017.04.040.

Park, E.-J., Park, S.-J., Kim, S., Lee, K., Chang, J., 2018. Lung fibroblasts may play an important role in clearing apoptotic bodies of bronchial epithelial cells generated by exposure to PHMG-P-containing solution. Toxicol. Lett. 286, 108–119. https://doi.org/10.1016/j.toxlet.2018.01.003.

Park, J.S., Park, Y.J., Kim, H.R., Chung, K.H., 2019a. Polyhexamethylene guanidine phosphate-induced ROS-mediated DNA damage caused cell cycle arrest and apoptosis in lung epithelial cells. J. Toxicol. Sci. 44, 415–424. https://doi.org/10.2131/jts.44.415.

Park, Y.J., Jeong, M.H., Bang, I.J., Kim, H.R., Chung, K.H., 2019b. Guanidine-based disinfectants, polyhexamethylene guanidine-phosphate (PHMG-P), polyhexamethylene biguanide (PHMB), and oligo(2-(2-ethoxy)ethoxyethyl guanidinium chloride (PGH) induced epithelial-mesenchymal transition in A549 alveolar epithelial cells. Inhal. Toxicol. 31, 161–166. https://doi.org/10.1080/08958378.2019.1624896.

Schug, T.T., Janesick, A., Blumberg, B., Heindel, J.J., 2011. Endocrine disrupting chemicals and disease susceptibility. J. Steroid Biochem. Mol. Biol. 127, 204–215. https://doi.org/10.1016/j.jsbmb.2011.08.007.

Shin, D.Y., Jeong, M.H., Bang, I.J., Kim, H.R., Chung, K.H., 2018. MicroRNA regulatory networks reflective of polyhexamethylene guanidine phosphate-induced fibrosis in A549 human alveolar adenocarcinoma cells. Toxicol. Lett. 287,

49–58. https://doi.org/10.1016/j.toxlet.2018.01.010.
Song, J., Kim, W., Kim, Y.-B., Kim, B., Lee, K., 2018. Time course of polyhexamethyleneguanidine phosphate-induced lung inflammation and fibrosis in mice. Toxicol. Appl. Pharmacol. 345, 94–102. https://doi.org/10.1016/j.taap.2018.02.013.
Yoon, H.M., Lee, E., Lee, J.S., Do, K.-H., Jung, A.Y., Yoon, C.H., Kim, S.-O., Jang, S.-J., Hong, S.-J., Cho, Y.A., 2015. Humidifier disinfectant-associated children's interstitial lung disease: computed tomographic features, histopathologic correlation and comparison between survivors and non-survivors. Eur. Radiol. 26, 235–243. https://doi.org/10.1007/s00330-015-3813-1.
Yoon, J., Cho, H.J., Lee, E., Choi, Y.J., Kim, Y.H., Lee, J.L., Lee, Y.J., Hong, S.J., 2017. Rate of humidifier and humidifier disinfectant usage in Korean children: a nationwide epidemiologic study. Environ. Res. 155, 60–63. https://doi.org/10.1016/j.envres.2017.01.030.
Zhang, J., Liu, L., Ren, L., Feng, W., Lv, P., Wu, W., Yan, Y., 2017. The single and joint toxicity effects of chlorpyrifos and beta-cypermethrin in zebrafish (Danio rerio) early life stages. J. Hazard Mater. 334, 121–131. https://doi.org/10.1016/j.jhazmat.2017.03.055.